Fracture 1977, Volume 3, ICF4, Waterloo, Canada, June 19 - 24, 1977

CRACK NUCLEATION IN 316 STAINLESS STEEL FUEL CLADDING

D. Lee*, R. A. Rand** and G. G. Trantina*

INTRODUCTION

Failure of nuclear fuel cladding is believed to depend largely on the process of crack nucleation caused by localized deformation at the pellet-clad interface in the presence of aggressive environments. It has been shown that some of the principal reactive fission products, including iodine, caused intergranular attack on stainless steel cladding [1] and iodine and tellurium, for example, promote surface nucleated cracking of stainless steels [2].

Since the failure is caused by the localized stresses and strains in cladding due to thermal expansion and cracking of fuel pellets as well as by the presence of fission products, it is necessary to identify the nature of interaction between the fuel and cladding. In order to achieve these objectives, several fuel rod modelling codes have been developed to describe the overall behaviour of fuel rods [3]. A physical model of the local strain and stress concentrations which occur in cladding due to the combined effect of radial cracks in the fuel and the frictional forces developed at the fuel-clad interface has also been proposed [4]. While a detailed finite element analysis based on this model has also been made [5], there has been no experimental verification of the models that have been proposed. Experimental methods of simulating pellet-clad interaction have been reported [6]; however, direct comparison with analytical models is difficult because of complex conditions that exist at the fuel-clad interface.

In order to simulate critical conditions that lead to the early stage of cracking, specially designed sheet tensile specimens were prepared so that the strain distribution in the sample would closely approximate that of cladding undergoing localized deformation. This was accomplished by using the finite element method to determine the strain distributions in the samples and by incorporating the results obtained from fuel rod modelling [5]. In this way, the local strains and strain distributions can be correlated and the effects of material variables as well as the details of the fuel cladding model can be directly related to the process of crack nucleation. Some of the results obtained with 316 stainless steel cladding materials are presented.

*General Electric Corporate Research and Development, Schenectady, New York 12301.
**Formerly with General Electric Corporate Research & Development, now at General Electric Boiling Water Reactor Systems Department, San Jose, California.

EXPERIMENTAL PROCEDURE

Materials

A type 316 stainless steel (13.6 Ni, 16.7 Cr, 2.52 Mo, 1.54 Mn. 0.5 Si, 0.13 Cu, 0.15 Co, 0.05 C, 0.010 P and .011 S with the balance Fe by weight percent) was tested in the 20% cold worked condition. This was produced by cold rolling a sheet stock of 3.2 mm to 1.70 mm followed by a solution treatment of 1100°C/10 min. plus water quench and a final rolling to 1.37mm.

Sample Design

Two types of test samples were prepared, as shown in Figure 1. The simple uniaxial test sample, Figure 1a, was used to produce the basic stress-strain curve used as input to the finite element analysis. The grooved sheet sample, Figure 1b, was designed based on calculations obtained from the fuel rod model. The details of the groove were designed so that the strain distribution in the sample would closely approximate that of cladding undergoing localized deformation due to interaction with the cracked fuel.

Testing Method

All the test samples were taken in the transverse direction of the rolled sheet and tested at 550°C. Simple uniaxial tension specimens were pulled at 4.2×10^{-3}mm/sec. corresponding to a strain rate of 1.1×10^{-4}sec.$^{-1}$ in air. Grooved specimens were tested at 4.2×10^{-4}mm/sec. so that the resulting strain rate is nearly comparable to that of simple uniaxial specimens. Iodine vapour was supplied to the test chamber by passing high purity helium through crystalline iodine which was kept at room temperature with resulting iodine partial pressure of 0.3 torr. True stress-true strain relationship was obtained with the extensometer attached in the axial direction; beyond necking, the minimum specimen section was measured by pointed micrometers.

ANALYTICAL PROCEDURE

The analysis of the grooved sheet was performed using the NONFIN finite element code [7]. The code has the capability of treating both flow and deformation theories of plasticity in an incremental fashion with a first order equilibrium correction. The present results will be restricted to infinitesimal theory and isotropic materials. The plane strain mode of deformation was used for the specimen analysis. The uniaxial stress-strain data was used as fifteen linear line segments thus providing an accurate representation of the actual experimental data.

The finite element grid used for the analysis of the grooved specimens has 14 quadrilateral elements (composed of four constant strain triangles) across the net section and a total of 260 nodes. The lower boundary is a plane of symmetry with no vertical displacement and at the upper boundary a uniform displacement is applied. The extraordinary length of the model (12.7mm) was necessary to allow for bending of the specimen. The results for models with shorter lengths resulted in a sensitivity of local strain to changes in length of the model. However, for the 12.7mm model, a change in length of the model results in insignificant change in local strain.

RESULTS AND DISCUSSION

Material Properties

The results of four uniaxial tensile tests are summarized in Figure 2 in the form of a true stress-true strain curve that includes the point of fracture. The maximum load was reached at the true strain of about 0.08; beyond that level of strain, the test specimen deformed in an unstable manner. The deviation from plastic isotropy was examined by comparing plastic strains in the width and thickness directions of the deformed samples. Since the plastic strain ratio was nearly unity, it is assumed that the material is isotropic in the plasticity analysis.

The flow strength was not markedly dependent on the strain rate; in fact, a negative strain rate sensitivity of flow stress has been observed in a few cases (Table I). The assumption that the material is insensitive to the strain rate appears to be justified for the specific testing condition.

Stress-Displacement Relationship

The stress-diplacement relationship for the grooved test specimen can be predicted by the finite element method using the uniaxial tension test data. In order to check the reliability of the finite element analysis method, a tension test was made with a grooved sample (Figure 1b) at 550°C. The displacement was measured with an extensometer attached over a 25.4mm gage length including the groove. The results of tests with two specimens are shown in Figure 3. The nominal stress is calculated as the load divided by the initial area of the net section at the groove.

In order to predict the stress-displacement results, a finite element analysis of the grooved specimen was made. The load was determined from the stresses at the boundary where the displacements are applied 12.7mm from the root of the groove. Since the analysis does not allow for finite deformation and since the maximum local strains were large (27%), it was necessary to decrease the load by the amount of area reduction at the groove as predicted by the finite element analysis. This resulted in a reduction in load of up to 6% at the end of the analytical stress-displacement curve. This load was then divided by the original net section area and the resulting curve is shown in Figure 3. The stress predicted by the analytical curve exceeds the experimental curve by less than 12% and by only 4% at the end of the curves. The difference can be attributed to the inability of the grooved specimen to achieve total plane strain conditions. The calculated axial strain at the root of the groove, as a function of the specimen displacement is also shown in Figure 3.

Comparison of Calculated Strain Distributions

By extending the finite element analysis technique to the fuel cladding [5], it is possible to identify conditions under which the strain distribution in the test sample match closely with that of the fuel cladding. For the purposes of illustrating a specific comparison of strain distributions in the test sample and the fuel cladding, an example from Reference 5 was chosen. The strain distribution for the cladding at a power level of 43 kW/m reached in 10 hours was compared with the strain distribution in the sample for a displacement of 0.05mm over the 25.4mm gage length. The maximum local strain for both cases was about 0.02. For this example, the strain distributions are similar with the strain gradient being somewhat more severe in the sample. For other fuel-cladding

conditions and power levels, the geometry of the sample can be modified, if necessary, to adequately simulate the strain distribution in the cladding.

The process of crack nucleation can therefore be related to the level of maximum strain and the specific condition of fuel cladding undergoing a similar mode of deformation. Thus, increasing the maximum strain or increasing the displacement in the test sample corresponds to increasing the level of power in the fuel rod.

Crack Nucleation Behaviour

When the grooved specimen was tested in air, no cracks were observed throughout deformation up to the point of fracture. Fracture took place by shear along about 45° to the loading direction, as shown in Figure 4a. The transition area from the original surface to the area of fracture, as shown in Figure 4b, indicates evidence of plastic deformation in the original surface. Elongated cuplets on the fractured surface are suggestive of a void nucleation and coalescence mechanism.

When the grooved specimen was tested in an iodine atmosphere, the specimen was loaded to several levels of load and the specimen examined under the microscope at a magnification of 700X. For stress levels of 335.0 MPa and 468.9 MPa corresponding to calculated local strains (Figure 3) of about 0.01 and 0.02 respectively, no cracks were observed. At a stress level of 602.2 MPa corresponding to a local strain of about 0.04, cracks were observed. The apperance of the specimen surface at low magnification is shown in Figure 4c. The high magnification SEM photograph in Figure 4d shows chemical reaction products on the surface near the cracks.

Accurate estimation of the conditions that will cause crack nucleation in fuel cladding requires precise modelling of fuel rod behaviour, well-defined experiments that simulate the critical features, and valid analysis of the experimental results. Additional work in these three areas is required to come to more accurate assessment of strain levels required for crack nucleation. Nevertheless, this work represents an attempt to develop a methodology to simulate crack nucleation in nuclear fuel cladding by laboratory testing coupled with finite element analysis.

CONCLUSIONS

1) Two important features that may be simulated in laboratory testing for failure of nuclear fuel cladding are localized deformation and the presence of fission products.
2) The finite element analysis method may be used as a general guide for designing laboratory specimens to simulate important features identified from the fuel rod modelling codes. Calculated local strain can be used as an estimate for strain where cracks nucleate.
3) In laboratory testing, 20% cold worked 316 stainless steel at 550°C fractured by shear mode and by void nucleation and growth process when deformed in air under near plane strain conditions. In the iodine atmosphere, cracks nucleated in multiple fashion and the surface near cracks were decorated by reactive products. The level of strain necessary for crack nucleation in the iodine environment was estimated to be about 0.04 based on results of a finite element analysis.

ACKNOWLEDGEMENTS

The authors would like to express their appreciation to H. J. Busboom of General Electric Breeder Reactor Operation for the material, P. T. Hill for all the mechanical testing, M. Gill for scanning electron microscopy work and M. D. German and C. F. Shih for consultation on the use of finite element analysis method.

REFERENCES

1. JOHNSON, C. E. and CROUTHAMEL, C. E., J. Nucl. Mat., 34, 1970, p.101.
2. LOBB, R. C. and JONES, R. B., Physical Metallurgy of Reactor Fuel Elements, Eds. Harris and Sykes, The Metals Society, London, 1975, p.27.
3. MATTHEWS, J. R., Advances in Nuclear Science and Technology, Academic Press, New York and London, 6, 1972, p.65.
4. GITTUS, J. H., Nucl. Eng. and Design, 18, 1972, p.69.
5. RAND, R. A., WILKINSON, J. P. D. and TRANTINA, G. G., Trans. of the 3rd Inter. Conf. on Structural Mech. in Reactor Tech., London, Sept. 1975.
6. WOOD, J. C., SURETTE, B. A., LONDON, I. M. and BAIRD, J., J. Nucl. Mat., 57, 1975, p.155.
7. LEE, D., SHIH, C. F. and TRANTINA, G. G., Plasticity Theories and Structural Analysis of Anisotropic Metals, EPRI Quarterly Report No. 2, General Electric Corporate Research and Development, Report SRD-75-116, Schenectady, New York, Nov. 1975.

Table 1 Effect of Strain Rate on Flow Stress

Initial Strain Rate sec^{-1}	True Stress, MPa		
	$\varepsilon^p = .002$	$\varepsilon^p = .02$	At Maximum Load
1.1×10^{-2}	539.0	613.7	641.9
1.1×10^{-4}	503.3	621.9	672.3
1.1×10^{-6}	524.0	615.7	675.7

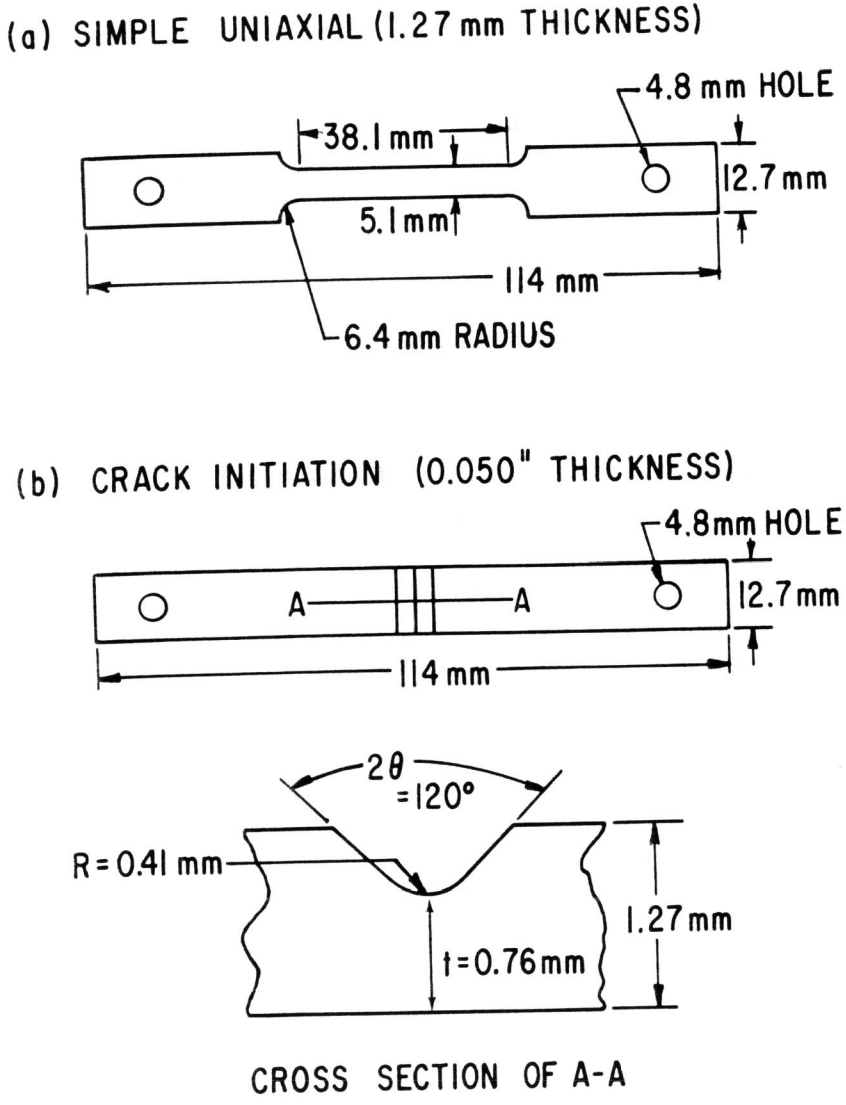

Figure 1 Details of Test Specimens

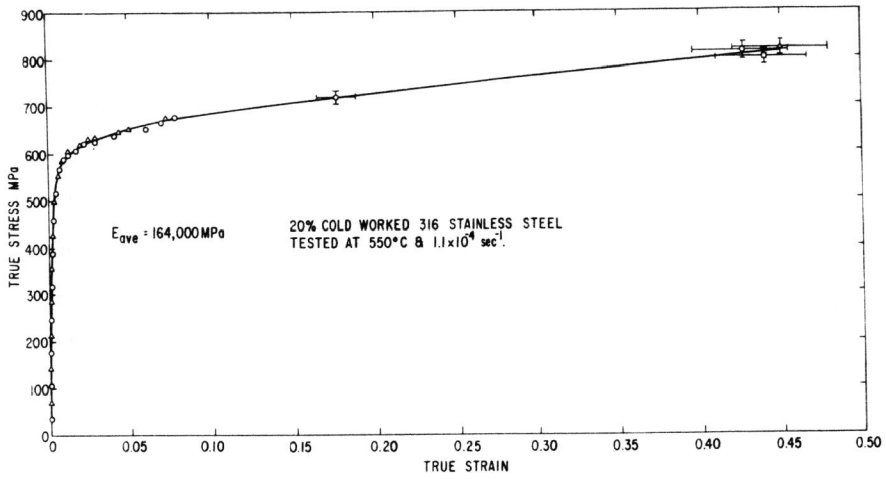

Figure 2 True Stress-True Strain Curves for 20% Cold Worked 316 Stainless Steel Tested at 550° C and 1.1 x 10^{-4} $sec.^{-1}$

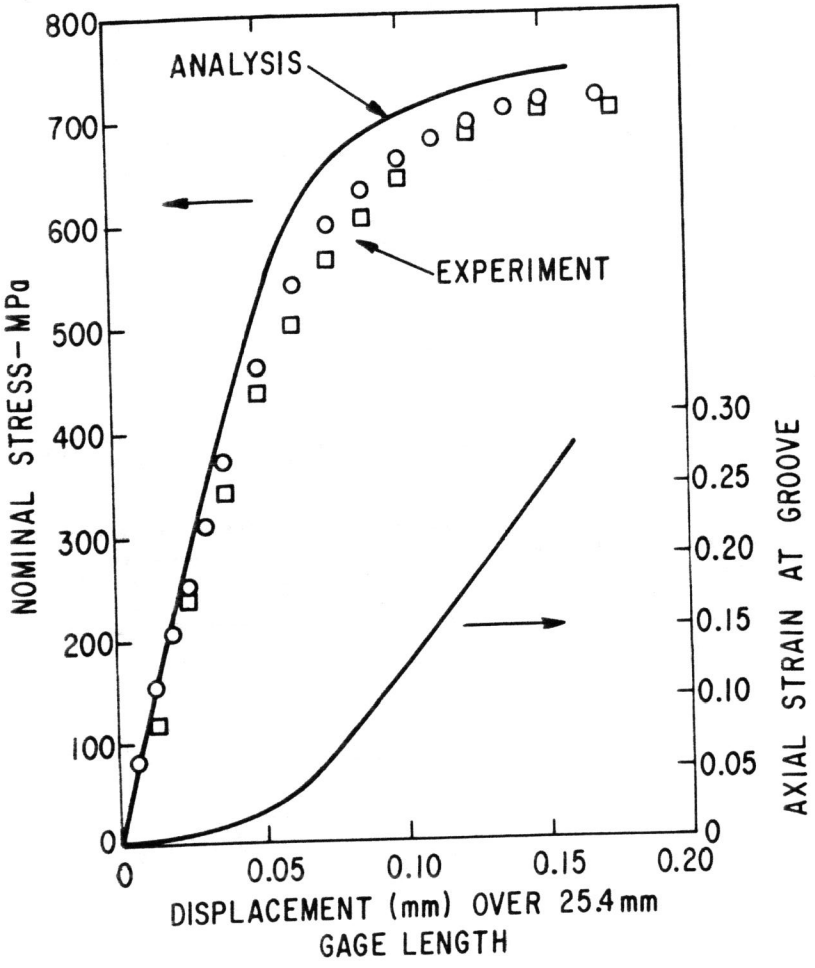

Figure 3 Nominal Stress and Axial Strain at Groove Versus Displacement for 20% Cold Worked 316 Stainless Steel Grooved Specimen Tested at 550° C. Experimental Data in Duplicate Tests are Shown by Circles and Squares

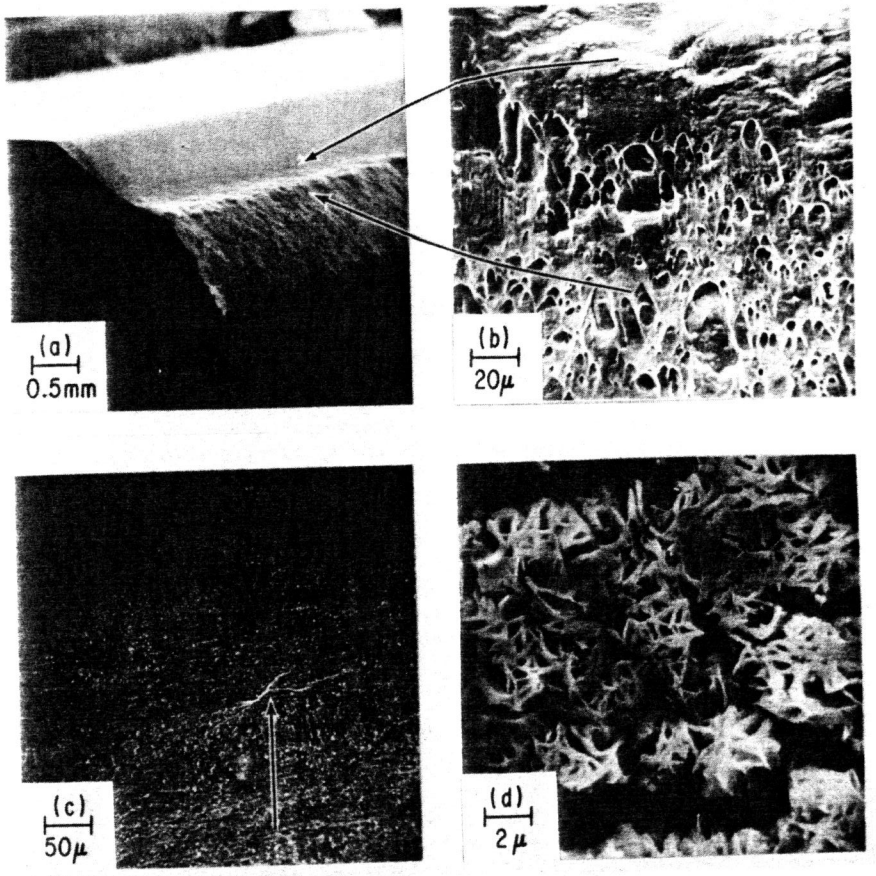

Figure 4 Scanning Electron Microscopy Photographs of Deformed and Fractured Grooved Specimens:

(a) Overall View of Specimen Fractured in Air
(b) Fractured Surface of (a),
(c) Appearance of Cracks for the Specimen Loaded to 602.2 MPa in Iodine, and
(d) High Magnification of Cracks Shown in (c)